THE ASTROPHYSICAL JOURNAL, 428:51–60, 1994 June 10

DARK MATTER AROUND A CLUSTER OF GALAXIES UNDER THE LONG COSMIC STRING SCHEME

TETSUYA HARA,[1] MASAKAZU MATSUURA,[1] HIDEKI YAMAMOTO,[1] PETRI MÄHÖNEN,[2] AND SHIGERU J. MIYOSHI[1]
Received 1993 May 14; accepted 1993 December 7

ABSTRACT

We study the formation of cluster of galaxies induced by cosmic strings in a flat universe dominated by cold dark matter. A cluster of galaxies is considered to be formed at the crossing site of three wakes of infinitely long cosmic strings. In this scheme, we investigate the distribution of dark matter and galaxies within and around a cluster of galaxies. The simulated line-of-sight velocity dispersion and projected surface number density of galaxies are compared with the observations in a simplified case. Some features seem to be in good agreement with the observation, although the detailed structures require a more refined investigation. A characteristic pattern of density inhomogeneities is expected to exist within a cluster, which might be related to the substructures observed in many clusters of galaxies. The brightest cluster member, such as a gE, D, or cD galaxy, is naturally expected to reside at the cluster center in this scheme.

Subject headings: cosmic strings — dark matter — galaxies: clustering

1. INTRODUCTION

There are several optical observational data bases of clusters of galaxies, and they yield the velocity dispersion, the surface number density of galaxies in and around individual cluster of galaxies (e.g., Dressler 1979; Kent & Gunn 1982; Millington & Peach 1986; Fitchett & Webster 1987; Ostriker et al. 1988; Dressler & Schectman 1988; Chapman, Geller, & Huchra 1989; Geller 1990; Beers et al. 1991). In addition, there are X-ray data of clusters of galaxies, which will strongly reflect the distribution of dark matter in each cluster (e.g., Forman & Jones 1982, 1990; Sarazin 1986; McMillan, Kowalsky, & Ulmer 1989; Edge et al. 1990; Buote & Canizaros 1992; Davis & Mushotzky 1993).

There has been a large number of works trying to explain such observations under the adiabatic perturbation scenario including the biasing effects. While they have many successes in explaining various features, some discrepancies still remain unsolved (Peebles & Silk 1990; Peebles 1990; Cavaliere & Colafrancesco 1990; West 1990; Kaiser 1990; Bahcall & Cen 1992). On the other hand, the cosmic string model (Kibble 1976; Vilenkin 1985) seems to have developed into one of the viable models accounting for such problems, and here we investigate the distribution of cold dark matter (CDM) around a cluster of galaxies and some related problems using this scheme. Although we adopt rather simplified assumptions, the simulated results seem to be in fairly good agreement with observations as shown below.

Our main ideas are that the galaxies were formed within or near the wakes formed in the trace of fast long cosmic strings (Silk & Vilenkin 1984) and that, if three wakes crossed each other almost orthogonally, matter (galaxies) has accumulated to the crossed point to form a cluster (Hara & Miyoshi 1989; Vachaspati 1986). Under such scheme, the CfA observation (Geller & Huchra 1989) has been compared with a simulated configuration of three orthogonally intersected wakes (Hara, Morioka, & Miyoshi 1990). Although we have to be careful to derive conclusions based on the visual comparisons, the similarity between the CfA observation and the simulation in cone diagrams seems to be good (Hara & Miyoshi 1993). The mass of cluster of galaxies ($\sim 10^{15}\ M_{\odot}$) has been obtained in this scheme (Hara & Miyoshi 1989). The number density, mass function, and correlation function of cluster of galaxies have also been investigated, including the velocity distribution of cosmic strings (Hara et al. 1994b).

Most prominent wakes are created when cosmic strings have passed through the universe at redshift $z \sim 10^4$ (Stebbins et al. 1987; Hara et al. 1993a). We therefore pay attention mainly to the wakes triggered at around this epoch and simulate the distribution of CDM around and within a cluster for some typical cases of three orthogonally intersecting wakes.

Properly stating, we should simulate the motion of cosmic strings over the horizon and then calculate the motion of dark matter from a stage of $z \gtrsim 10^4$ up to the present, taking into account the effect of small-scale structure of long strings (Stebbins 1988; Bouchet, Bennett, & Stebbins 1988). Such a simulation, however, seems to have too many free parameters, and the numerical results of string motion are now still subjects of lively debate on the amount, generation, and scale of the structure both on loops and long strings (Albrecht & Turok 1989; Bouchet & Bennett 1990; Allen & Shellard 1990; Copeland, Kibble, & Austin 1992). Hence it is difficult to simulate the motion of dark matter in general situation. Therefore, for the moment, we adopt a simple toy model to examine whether the cosmic string model could explain the characteristic features of the clusters of galaxies or not.

In this paper, we are concerned mainly with the distribution of dark matter around and within a cluster of galaxies, and we calculate the motion of dark matter for the formation of cluster of galaxies under rather simplified situation of strings. Although the distribution of dark matter should be calculated with a much more refined program or with a denser mesh than we used, we believe that some characteristic features of dark matter distribution around a cluster are well described. We do not consider the effects of the cosmic loop strings in this paper; however, they should be included in more realistic simulations (Sato 1986; Bertschinger 1988; Brandenberger 1990; Batsuki et al. 1991). We treat cold dark matter in this paper and leave the

[1] Department of Physics, Koyoto Sangyo University, Kyoto 603, Japan.
[2] Department of Astrophysics, University of Oxford, Oxford, UK; also Department of Theoretical Physics, University of Oulu, Oulu, Finland.

more complicated problem with respect to hot dark matter (HDM) to subsequent papers.

In § 2 we describe in detail the adopted situation. Then we present in § 3 the distribution of dark matter and galaxies around and within a cluster obtained from simulations, where we compare the radial distribution of velocity dispersion and surface number density of galaxies with observations. The object formed in the center of a cluster is discussed in relation to a cD galaxy in § 4. The problems remaining in our treatment are discussed in § 5.

2. ASSUMPTIONS AND EQUATIONS OF MOTION OF DARK MATTER

We consider that an infinitely long straight cosmic string has passed at an epoch of redshift z_i and assume that a wake is formed behind the trace of the string. The distance, Δx, that a dark matter particle moves toward the wake until the present has been estimated analytically (Hara et al. 1993a; Stebbins et al. 1987) as shown in Figure 1. The length Δx depends on the parameters as $\Delta x \propto (G\mu\beta\gamma/3 \times 10^{-6})$, where μ and β are the line mass density and the velocity of cosmic string in units of $c = 1$, respectively, and $\gamma = (1 - \beta^2)^{-1/2}$. The distribution of dark matter within a wake has been calculated with 6×10^3 particles in the case of one-dimensional contraction, as shown in Figure 2 (Hara et al. 1993a). The height Δh of the wake is approximately $\Delta h \simeq 0.15 \times \Delta x$. This length also roughly corresponds to the characteristic radius of cluster of galaxies simulated in the three-dimensional case described later.

Here we calculate the motion of CDM in the configuration that three cosmic strings passed through and triggered the formation of three orthogonally crossing wakes at $1 + z = 10^4$. The equation of motion of CDM particle in the flat Friedmann universe is given by

$$d^2\boldsymbol{x}/dt^2 = -2a^{-1}(da/dt)d\boldsymbol{x}/dt - a^{-3}\nabla_{\boldsymbol{x}}\Phi\,, \qquad (1)$$

where $\boldsymbol{x}$ is the particle position in the comoving coordinates and $a(t)$ is the scale factor of the universe. The peculiar gravitational potential Φ satisfies the Poisson equation

$$\Delta\Phi = 4\pi G a(t)^3(\rho - \rho_b)\,, \qquad (2)$$

where ρ and ρ_b are the density and background density of CDM. The time evolution of $a(t)$ is governed by

$$a^{-2}(da/dt)^2 = 8\pi G\rho_{\rm eq}[(a_{\rm eq}/a)^4 + (a_{\rm eq}/a)^3]\,, \qquad (3)$$

where $a_{\rm eq}$ and $\rho_{\rm eq}$ are the values of a and ρ_b at the matter-radiation equality era.

In principle, we treat the dark matter only. When we need to consider the distribution of galaxies, we consider a fraction f of particles as galaxies which satisfy either of the following criteria: (1) particles reside in a wake within a height h (~ 1 Mpc) (thickness is $2h$), (2) particles situate within a radius r (~ 1.5 Mpc) from the cluster center. The derived results resemble each other, even if the values of h and r are fairly changed or if galaxies are set to distribute in proportion to dark matter.

At first we investigate the case that three wakes intersected orthogonally like the x-y, y-z, and x-z planes in the Cartesian coordinates. We calculated also the cases that the intersected angles are deviated from 90° by $\Delta\theta$ ($\sim 15°$) and found that the changes in characteristic features were small. Even in the case that all wakes were triggered at different epochs, such as $1 + z_i = 3 \times 10^4$, 10^4, and 3×10^3, respectively, the characteristic features remained almost unchanged. The reason for the small changes in the latter case is that the induced velocity difference is so small that a relatively small difference in trigger time does not lead to great differences in results.

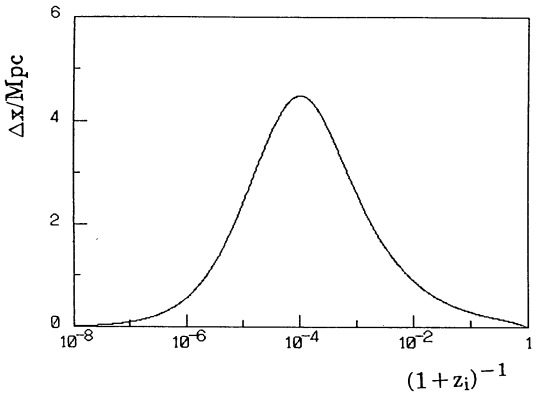

FIG. 1.—Deviation length vs. triggered epoch $1 + z_i$. The deviation length Δx of dark matter due to the wake triggered at the epoch of redshift $1 + z_i$ is displayed in case of one-dimensional contraction with $G\mu\beta\gamma = 3 \times 10^{-6}$.

To compare the results of simulation with the observations of Coma cluster (Kent & Gunn 1982; Millington & Peach 1986), we adopted the value $G\mu\beta\gamma = 5 \times 10^{-6}$ in the following analysis. The numerical calculations are made with the PM method with CIC mass assignment scheme, using 64^3 particles and cells (Hockney & Eastwood 1981; Efstathiou et al. 1985). We use the logarithmic time to follow the expansion of the universe between $z = z_i$ and 0 (Hara & Miyoshi 1993; Hara et al. 1993a). This numerical calculation is clearly a low-resolution one. However, we tentatively ran two comparison codes using 128^3 particles and 300^3 cells and found that a low-resolution result reported in this paper is qualitatively the same as those of comparison codes. Even in quantitative analysis they seem to be in fairly good agreement. The string energy density, μ, and coherent velocity, β, should be derived from realistic cosmic string network simulations. It is rather widely accepted that $G\mu \sim 2 \times 10^{-6}$ and $\beta \sim 0.15$ (Bouchet &

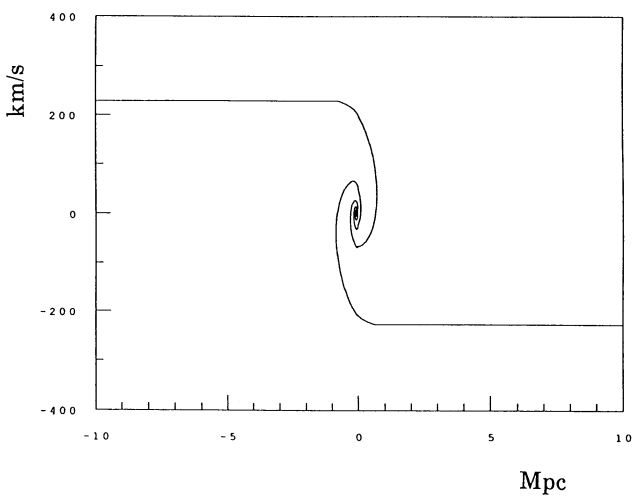

FIG. 2.—The peculiar velocity of CDM vs. the proper distance from the middle wake plane x. The phase space distribution of CDM particles falling toward the wake at present ($1 + z = 1$) is shown. The thickness $2\Delta h$ of the wake is $\sim 1.5(G\mu\beta\gamma/3 \times 10^{-6})$ Mpc. This is the case for one-dimensional contraction.

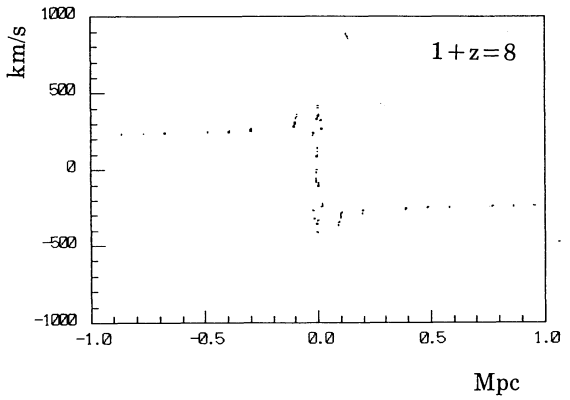

FIG. 3*a*

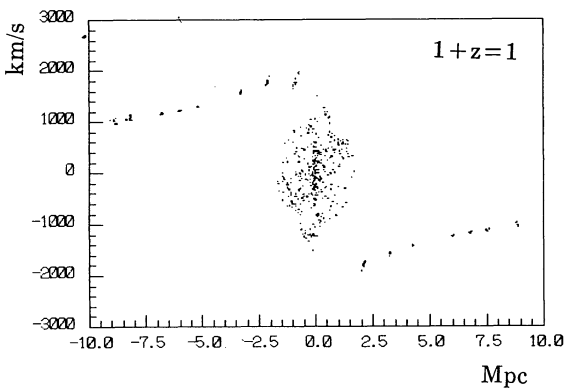

FIG. 3*c*

FIG. 3.—The peculiar-velocity distribution in a selected direction. Typical peculiar velocity distribution of CDM particles in a selected, say x-direction is presented. A total of 1000 particles initially situated around and along the x-axis are selected, and a part of them are plotted for different epochs of (*a*) $1 + z = 8$, (*b*) 2, and (*c*) 1. The vertical axis is the peculiar velocity in the x-direction and the horizontal axis shows the x-coordinates in the proper scale. The value of $G\mu\beta\gamma$ is 5×10^{-6}.

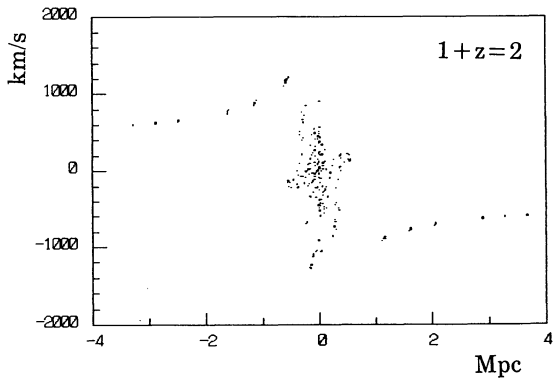

FIG. 3*b*

Bennett 1990; Allen & Shellard 1990), and our own independent code also gives similar results. The value adopted in this paper, $G\mu\beta\gamma = 5 \times 10^{-6}$, seems to correspond to rather high parameter values. However, the reason of the choice of this high value is that, since we do not include the small-scale structure of cosmic string in our toy model, the effective energy density of string must be higher for distant observer. On the other hand, it is said that there is an occasional cosmic string with high-velocity ($\beta \sim 1$) (Vachaspati & Vilenkin 1991; Shellard & Allen 1990), and it is seen also in our own code. Typically, the CDM particles move the distance of $\Delta x \sim 8(G\mu\beta\gamma/5 \times 10^{-6})$ Mpc in the case of one-dimensional contraction to the wake triggered at $1 + z = 10^4$. Hence we have to calculate in a region with comoving size of at least 30 Mpc in order to take into account all the effects of three-dimensional configuration of intersecting three wakes. We have calculated for several cases. Usually we take the comoving box length to be 48 Mpc, so that the comoving mesh box size, R_0, is 0.75 Mpc for the chosen parameter value of $G\mu\beta\gamma = 5 \times 10^{-6}$.

It must be noted that, once the configuration and initial stages are settled, the numerical calculation itself depends only on one parameter $V_1 = (G\mu\beta\gamma/5 \times 10^{-6})/(R_0/0.75\ \mathrm{Mpc})$ (Hara et al. 1993a). Therefore, the results obtained for a fixed value of V_1 are available for any case of $G\mu\beta\gamma = 5 \times 10^{-6}F_1$ and $R_0 = 0.75F_1$, where F_1 is an arbitrary factor. Accordingly, the particle velocity scales as $v \propto G\mu\beta\gamma \times R_0 \propto V_1 \times F_1^2$ and the mass of each particle amounts to $3.0 \times 10^{10} \times F_1^3\, M_\odot$.

3. VELOCITY AND DENSITY DISTRIBUTIONS

3.1. *Velocity Distribution in a Selected Direction*

Many CDM particles fall toward the crossing site of three wakes. Since it is not easy to describe the three-dimensional motion of particles falling from different directions as a whole, a typical velocity distribution of particles in one direction is presented in Figure 3. A set of 10^3 particles initially situated at around the x-axis are picked up and a part of them are plotted in Figures 3*a*, 3*b*, and 3*c* for different epochs of $1 + z = 8$, 2, and 1, respectively. The vertical axis is the peculiar velocity in the x-direction and the horizontal axis shows the x-coordinates in the proper scale. If we use many more particles and a smaller mesh size, the velocity distribution should become a convoluted one, as shown in Figure 2.

As seen from these figures, the turn-around length is $\sim 1.5(G\mu\beta\gamma/5 \times 10^{-6})$ Mpc at present, and many particles are accumulated within this length. It could be inferred that there is a characteristic radius for each cluster, which can be seen in the density profile described below. This characteristic length is consistent with that derived from the one dimensional infall shown in Figure 2. The infall velocity is $\sim 10^3(G\mu\beta\gamma/5 \times 10^{-6})$ km s^{-1}. This is different from that in the one-dimensional case shown in Figure 2, $\sim 400(G\mu\beta\gamma/5 \times 10^{-6})$ km s^{-1}. It may reflect the difference in the mass accumulated to the cluster center.

3.2. *Density vs. Radius in Spherical Approximation*

The simulated distribution of dark matter in and around a cluster is not spherically symmetric as described below. As the first approximation, we have derived the averaged radial distribution of dark matter in spherical symmetry. Thus obtained radial distribution of CDM volume density is given in Figure 4*a*, which shows $\rho \propto r^{-2}$ at $r \lesssim 2$ Mpc and decreases appreciably at $r \gtrsim 2$ Mpc. Thus the cluster potential is expected to have a characteristic radius in this model.

To compare it with the observations of galaxies, we have selected the points that satisfy either of the criteria (1) or (2) mentioned in § 2. The radial distribution of galaxies, obtained by assuming that 10% of CDM particles thus selected form galaxies ($f = 0.1$), is also shown in Figure 4*a* by a long-dashed

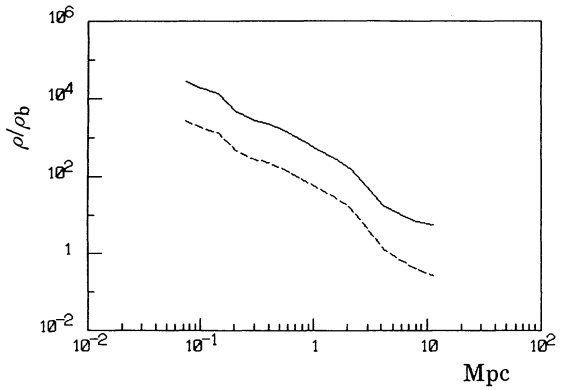

FIG. 4*a*

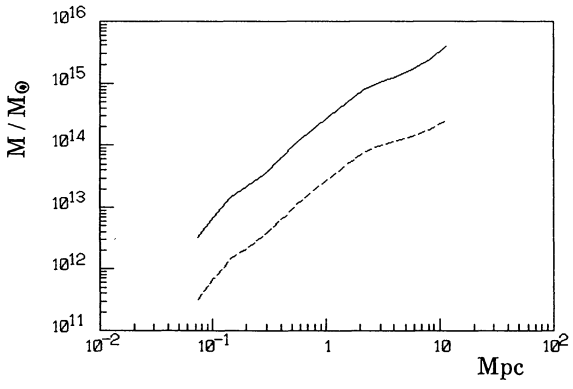

FIG. 4*b*

FIG. 4.—Space density vs. radius in spherical approximation. (*a*) The radial density distribution of CDM is shown by solid curve. The distribution of galaxies which satisfy either of the criteria (1) or (2) in case of $f = 0.1$ is also shown by the long dashed curve. (*b*) The mass of dark matter and galaxies within the radius r are shown by *solid* and *long-dashed curves*, respectively.

line. The masses of dark matter and galaxies within radius r are shown in Figure 4*b* by solid and long-dashed lines, respectively. The mass of dark matter within 1.5 Mpc is $\sim 10^{15}(G\mu\beta\gamma/5 \times 10^{-6})^3\ M_\odot$, which is comparable to that of Coma cluster (Hughes 1989).

3.3. *Comparison with Observations*

The projected radial distribution of surface density and velocity dispersion obtained by our simulation are compared with those observed for Coma cluster (Millington & Peach 1986) in Figures 5*a* and 6*a*, respectively. Since the configuration is not spherically symmetric, the direction of the projected plane should be suitably selected. We took the configuration investigated before (Hara & Miyoshi 1993) and the direction of normal vector of the projected plane was taken as $(\theta, \phi) = (130°, 8°)$, where θ and ϕ are the rotation angles in the spherical coordinates.

In Figure 5*a*, the background number density is taken to be 425 galaxies deg^{-2}. Although the details are slightly different, the overall observed features are well reproduced. To adjust the simulated number density of galaxies with the observation, we need to select one per 33 particles satisfying either of the criteria (1) or (2) as galaxies, which is denoted as $M/L = 33$. This means that the mass-to-luminosity ratio of the cluster is 33 times that of galaxies ($\sim 10\ M_\odot/L_\odot$).

In Figure 6*a*, the simulated velocity dispersion in the projected direction and the three-dimensional velocity dispersion are plotted by solid and long-dashed lines, respectively. The decrease in velocity at central part and the constant feature in the outer region are reproduced. If the observation is free from the contamination of foreground and background galaxies, there is a feature which cannot be reproduced under this simplified model. From a standpoint supporting the cosmic string scenario, it is suggested that a merging occurs in the central region of the Coma cluster, although we do not consider here the detailed structure of the Coma cluster (Fitchett & Webster 1987; Davis & Mushotzky 1993).

By way of suggestion, the simulated surface density and velocity dispersion for the projection angle $(\theta, \phi) = (45°, 45°)$ are shown in Figures 5*b* and 6*b*, respectively. Comparison with Figures 5*a* and 6*a* shows that the change in the surface number density with the projection angle is less than that of velocity dispersion. It is noted that the velocity dispersion for this projection angle gradually increases up to the radius $r \sim 6$ Mpc.

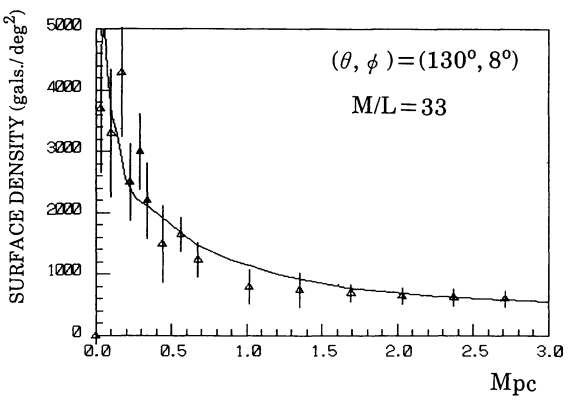

FIG. 5*a*

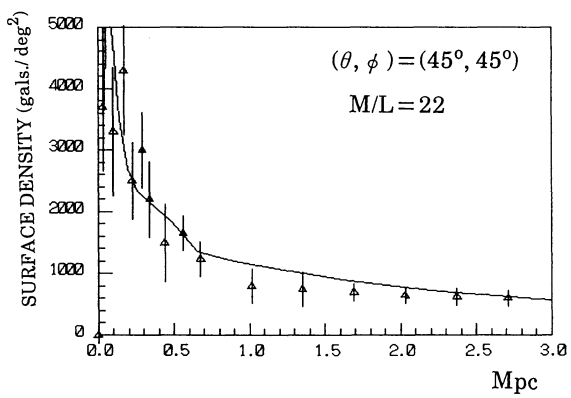

FIG. 5*b*

FIG. 5.—Surface density vs. projected radius. (*a*) The projected radial distribution of surface number density of galaxies is shown. We selected one per 33 particles satisfying either of criterion (1) or (2) as a galaxies and indicate it as $M/L = 33$. The normal vector of the projected plane is taken as $(\theta, \phi) = (130°, 8°)$ in the spherical coordinates. The adopted background number density of galaxies is 425 galaxies deg^{-2}. Triangles with error bars show the observed values of Coma cluster (Millington & Peach 1986). (*b*) The case for the projected direction $(\theta, \phi) = (45°, 45°)$.

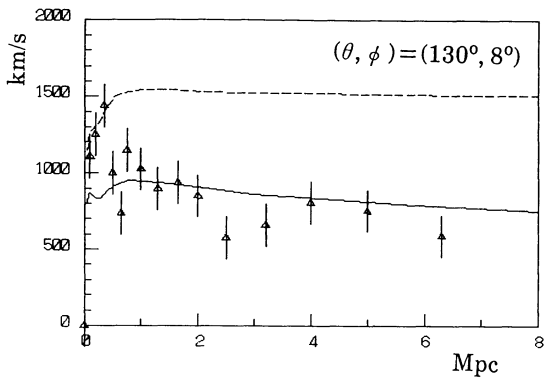

FIG. 6a

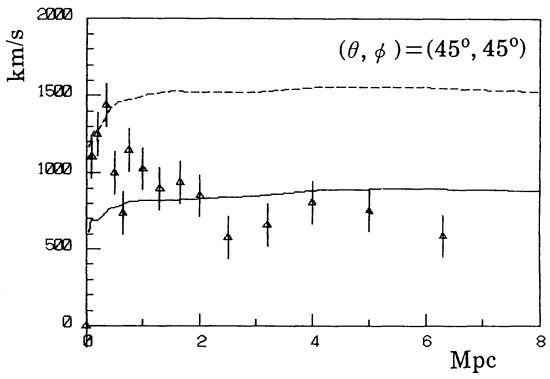

FIG. 6b

FIG. 6.—Radial distribution of velocity dispersion. (*a*) The velocity dispersion in the projected direction and three-dimensional velocity dispersion are depicted by *solid* and *long-dashed lines*, respectively. (*b*) The case changed with projected direction as $(\theta, \phi) = (45°, 45°)$ is shown.

3.4. *Change in Velocity Distribution with Projection Angle*

The change in velocity distribution of galaxies with projection angles is shown in Figure 7. A total of 2000 galaxies are plotted in each diagram. The case of $(\theta, \phi) = (90°, 0°)$, in which the observer is on the x-axis and far away from the center, is shown in Figure 7*a*. It shows two linelike concentrations indicating that many galaxies are moving toward or receding from the observer. The case of $(\theta, \phi) = (45°, 45°)$ is presented in Figure 7*b*, which shows no such pattern.

In the case of $(\theta, \phi) = (130°, 8°)$, found as the most suitable for the large-scale distribution of galaxies around the Coma cluster (Hara & Miyoshi 1993), the result is presented in Figure 7*c*, which also shows no apparent linelike pattern. The observational result is shown in Figure 7*d* (Kent & Gunn 1982; de

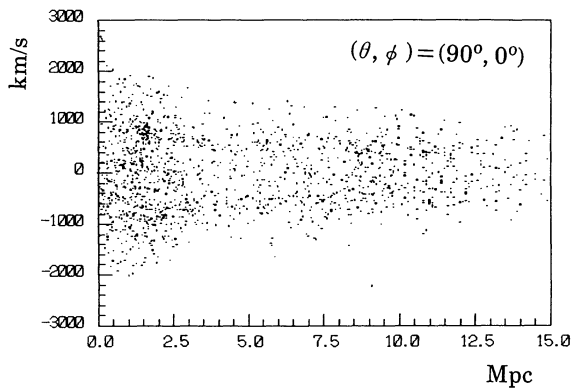

FIG. 7a

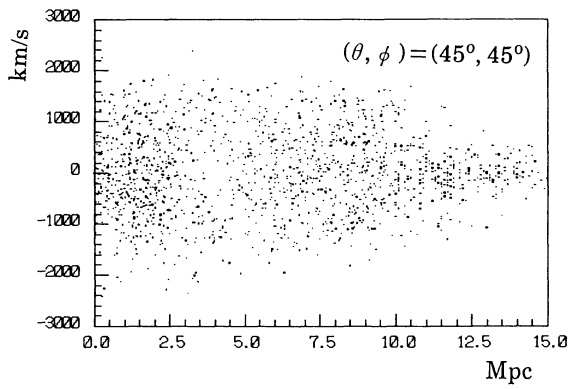

FIG. 7b

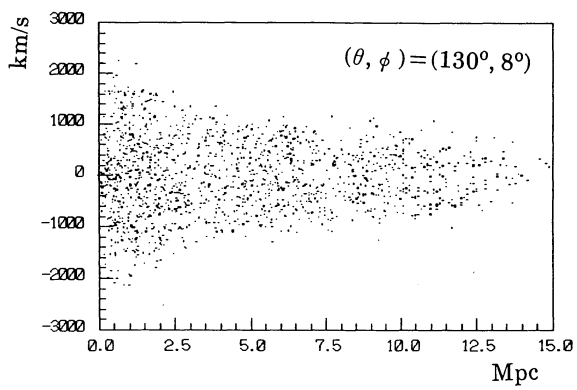

FIG. 7c

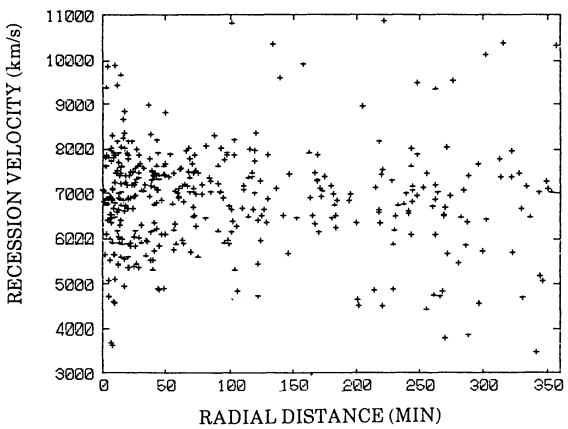

FIG. 7d

FIG. 7.—Velocity distributions for various projected directions. (*a*) The velocity distribution for a case of the projected direction $(\theta, \phi) = (90°, 0°)$ that the observer is on the x-axis is shown with 2000 galaxies. (*b*) The case of the projected direction $(\theta, \phi) = (45°, 45°)$ is shown. (*c*) The case of the direction $(\theta, \phi) = (130°, 8°)$ as expected from the large-scale distribution of galaxies around Coma cluster is shown. (*d*) The observed data of Coma cluster where 38 points of data are added from the Third Reference Catalogue of Bright Galaxies (de Vaucouleurs et al. 1991) to the main data (Kent & Gunn 1982). The 100′ correspond to 4.1 h_{50} Mpc.

Vaucouleurs et al. 1991). The resemblance between the simulation and the observation is best for $(\theta, \phi) = (130°, 8°)$.

3.5. *Isodensity Contours of Dark Matter around and within a Cluster*

The simulated present-day distribution of dark matter around and within a cluster is displayed in Figures 8 and 9, where the local to background density ratio ρ/ρ_b is used to discriminate the isodensity contours. The isodensity contours of $\rho/\rho_b = 4$, 20, 64, and 256 are displayed in Figures 8*a*–8*d*, and the isodensity contours of $\rho/\rho_b = 384$, 512, 768, and 1536 are displayed in Figures 9*a*–9*d*. The box size is 48 Mpc in Figures 8*a*–8*c*. The central region is magnified by 4 times in Figures 8*d* and 9; that is, the box size is 12 Mpc.

As expected, dark matter has accumulated to the three wakes as seen in Figure 8*a*. The density is higher in each barlike intersected region of two wakes as seen in Figures 8*b*–8*d*, and 9*a*. It can be understood that dark matter falls into each wake and at the same time accumulates toward the barlike intersected region. A considerable portion of CDM particles in the barlike part contract toward the center and form a cluster there.

It must be noted that there are considerable density inhomogeneities around and within a cluster of galaxies. Figures 9*a*, 9*b*, and 9*c* each show a total of six horns or lumps, reflecting the structure of the three crossing bars seen in Figures 8*b*–8*d* and 9*a*. Although there is a severe resolution limitation in our simulation for the structures of sizes less than ~ 1 Mpc, it is naturally expected that such density inhomogeneities could extend into the much smaller sizes as far as we adopt the CDM-dominant universe. The motion of dark matter is determined by the initial condition and the relatively dense barlike part of dark matter falls into the center. Dark matter passes through the center and returns. Such features are also derived in the case that three wakes intersected with crossing angle $\sim 75°$ and in the case that wakes were triggered at different epochs as $1 + z = 3 \times 10^4$, 10^4 and 3×10^3.

It has been reported that there are substructures in the distribution of hot gas and galaxies in many clusters of galaxies (e.g., Geller & Beers 1982; Tonry 1985; Fitchett & Webster 1987; Dressler & Shectman 1988; Geller 1990; Forman & Jones 1990; Buote & Canizares 1992). Judging from their observed substructures they might be considered to be caused by merging. However, our simulation shows that such substructures should be related also to the large-scale inflow of CDM and galaxies into the cluster. With respect to this problem, it is interesting to note that multiple sites of high-density regions are observed in some clusters such as A98,

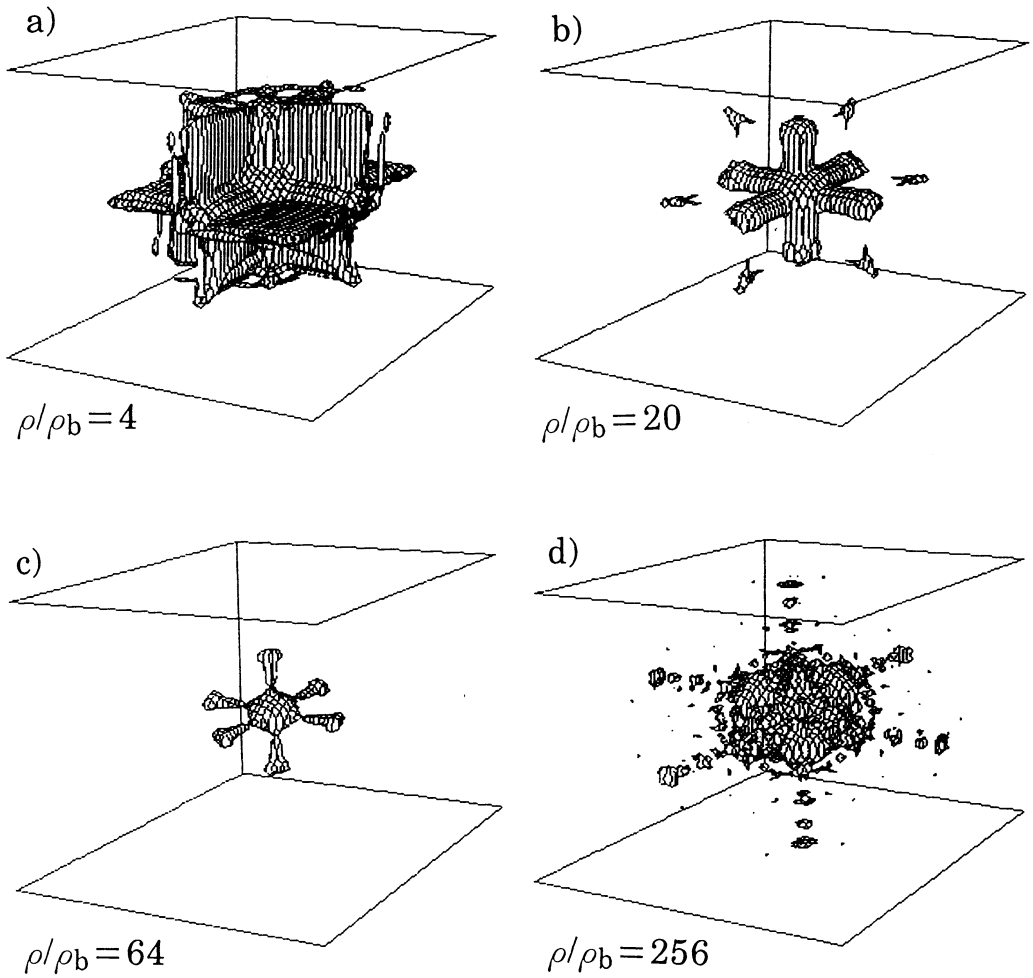

FIG. 8.—Isodensity contours of dark matter around and within a cluster. The quantities ρ/ρ_b is used to discriminate the isodensity contours. The isodensity contours of $\rho/\rho_b = 4$, 20, 64, and 256 are displayed in (*a*)–(*d*). The box size is 48 Mpc in (*a*)–(*c*) and 12 Mpc in (*d*).

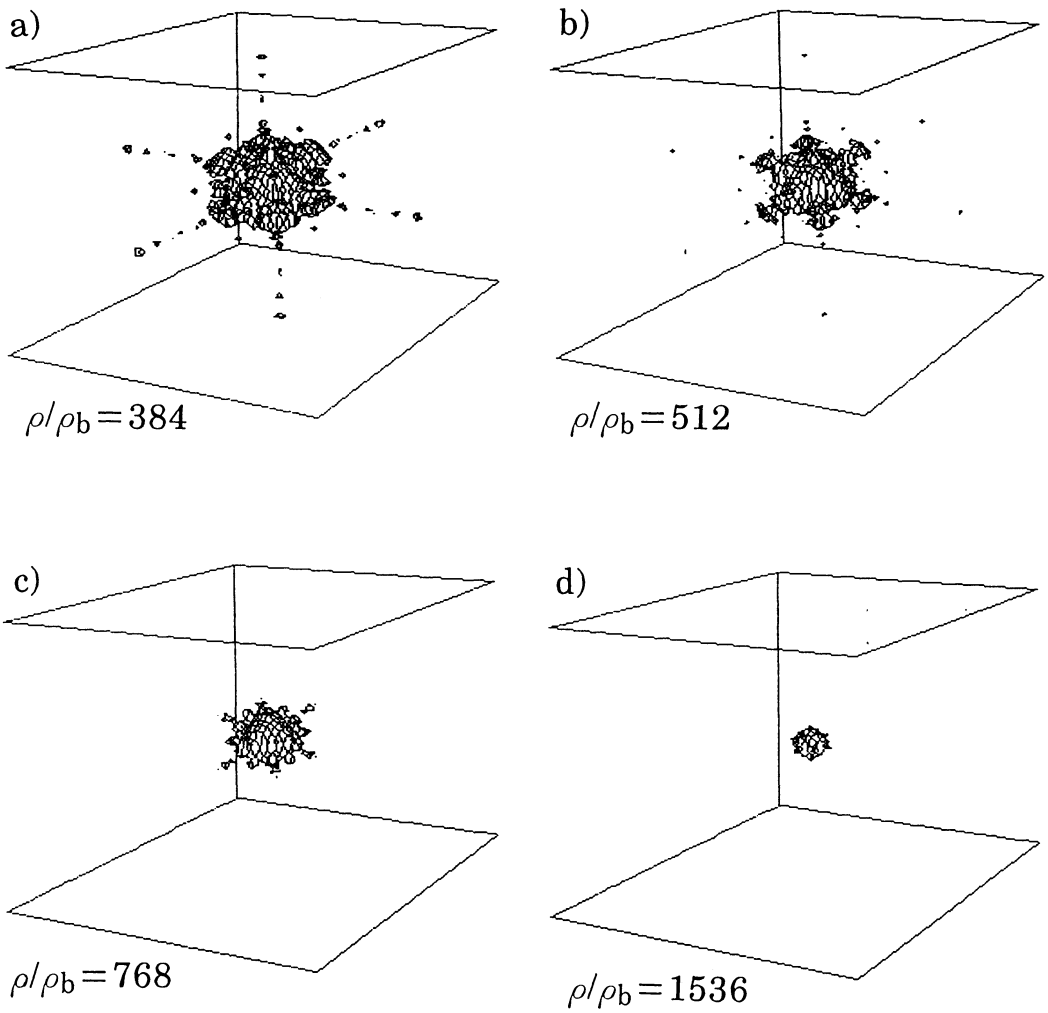

FIG. 9.—The same as Fig. 8 except the values of ρ/ρ_b. The isodensity contours of ρ/ρ_b = 384, 512, 768, and 1536 are displayed in (*a*)–(*d*). The box size is 12 Mpc.

A119, A2151, DC0622-64, and A1656 (Coma cluster) (Geller & Beers 1982; Geller 1990) which are shown in Figure 10. The bar to the upper left represents 0.48 h_{50}^{-1} Mpc at the cluster distance. The isodensity contour of Figure 9*b* with $\rho/\rho_b = 512$ is also shown there for the comparison. However, it is difficult to insist on the existence of such simulated structures (seven sites) from the observed surface number of galaxies because of the limited observed numbers and their discreteness. Although we should be very careful to derive any conclusion based on such visual impressions, it seems better to discern such structures by detailed X-ray surface observations which may reflect the distributions of hot gas in the inhomogeneous gravitational potentials. The temperature of such structures is roughly estimated as

$$T \simeq (8\pi/9)Gm_H(\rho/\rho_b)\rho_b r^2/k_B$$
$$\simeq 10^7[(\rho/\rho_b)/400](r/0.3\ \mathrm{Mpc})^2\ \mathrm{K}\ ,$$

where the relations $3kT/2 \simeq GMm_H/r$ and $M = 4\pi\rho r^3/3$ are used and m_H is the hydrogen mass. This value is consistent with those obtained from the X-ray observations of clusters of galaxies (Yamashita 1992). However, it must be stressed that the central potential is dominant among those of the multiple substructures.

4. cD GALAXY IN CLUSTER OF GALAXIES

The existence of the brightest cluster member (BCM) such as a gE, D, or cD galaxy at the cluster center is expected in this model. For a rich cluster, where three wakes are considered to intersect with each other almost orthogonally, a massive object is expected to form at the center of the cluster at an early stage of the universe ($1 + z \geq 8$). The time evolution of the mass M within a radius $3/(1 + z)^2$ Mpc and that of the velocity dispersion therein v_d are shown in Figure 11. The time change of the turn-around radius in the form $\sim(1 + z)^{-2}$ is expected from the analysis of one-dimensional contraction of CDM system (Hara et al. 1993a). As expected from this, $M \propto (1 + z)^{-3}$ and $v_d \propto (1 + z)^{-1/2}$.

The formation of objects corresponding to galaxies is expected to occur at around or after the epoch of redshift $1 + z \simeq 8$, when the Compton cooling time became longer than the expansion time of the universe. Before $1 + z \simeq 8$, if baryons happened to be hot and ionized, the Compton cooling was effective enough to cool the cosmic baryon temperature to the background radiation temperature, and therefore the Jeans mass remained much smaller than the galaxy mass. At around $1 + z \simeq 8$ the baryon gas temperature started to increase, if appropriate heating sources existed, and the Jeans mass of the

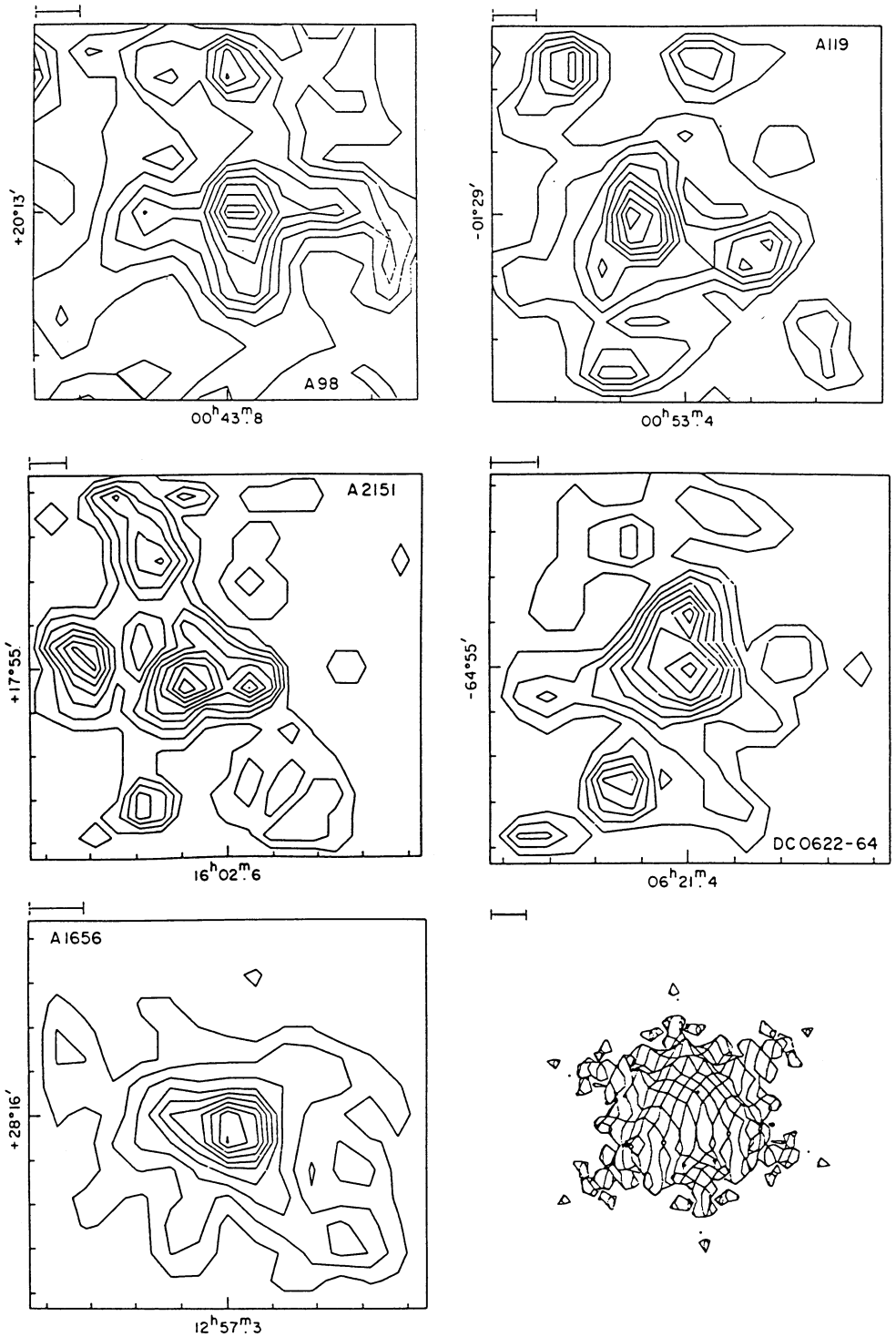

FIG. 10.—Galaxy surface number density contour diagram (Geller & Beers 1982) (*a*) A98, (*b*) A119, (*c*) A2151, (*d*) DC0622-64, (*e*) A1656 (Coma Cluster), (*f*) the same of Fig. 9(*b*) with $\rho/\rho_b = 512$. The bar to the upper left represents 0.48 Mpc at the cluster distance.

gas increased with this temperature as

$$M_J \simeq 3 \times 10^{10}[(T/10^4\ \mathrm{K})/(1+z)/8]^{3/2}[(\Omega_b/0.1)]^{-1/2}\, M_\odot \quad (4)$$

where Ω_b is the baryon density parameter.

The baryonic objects corresponding to the above Jeans mass are expected to form in a potential well of dark matter of which mass is greater than the Jeans mass M_J, because the gravitational inhomogeneities are governed mainly by dark matter. At $1 + z \simeq 8$, the radius and mass of the site, where three wakes intersected, are ~ 50 kpc and $\sim 10^{12}\, M_\odot$ as seen in Figure 11. Then a large galaxy could be expected to form at the cluster center. However, this is a rough picture, and detailed investigations of thermal process including both cooling and heating must be done through its evolution. In addition the similarity

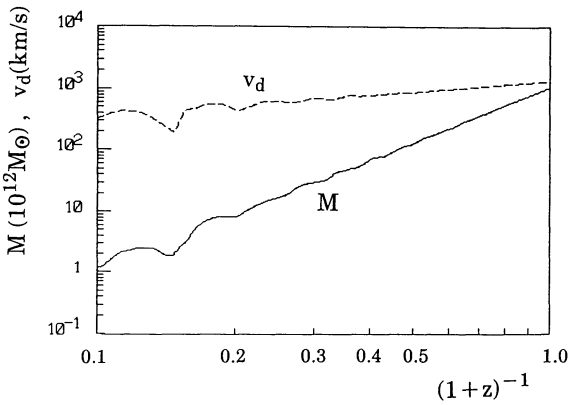

FIG. 11.—Cluster mass and velocity dispersion vs. $1 + z$. The time evolutions of mass M (*solid curve*) and velocity dispersion v_d (*dashed curve*) within a radius of $3/(1 + z)^2$ Mpc are shown. The oscillations of curves are due to the fluctuations in numerical calculation.

in structure between the central cD galaxy and the whole cluster (Tonry 1987) is expected, because the motion of dark matter toward each wake is already determined at around $1 + z \simeq 10^4$, when cosmic strings passed through. The intersection angle among three wakes and the magnitude of the infall velocity toward each wake are the same or correlated for the center galaxy and the whole cluster of galaxies. Then the several features such as major axes of the center galaxy are expected to correlate with that of the parent cluster (Binggeli 1982; Tonry 1987).

Moreover, it is also naturally expected that the center galaxy (BCM) is stationary at the cluster center, as long as it has not experienced merging (Quintana & Lawrie 1982; Tonry 1987). The cusplike distribution of matter in the center (Beers & Tonry 1986) and the nonrotating velocity distribution of stars in the cD galaxy could be also expected when the shape of whole cluster is not deformed. The decrease in velocity dispersion at the center of cD galaxy (Dressler 1979) as well as in the host cluster itself is also expected (see Fig. 6), since the dark matter gradually accumulates in the center of the cluster.

5. DISCUSSION

As mentioned above, there is a possibility that many observed features in clusters of galaxies could be explained by a simplified model of cosmic strings. However, the relation between the dark matter and galaxies is not yet fully understood. The detailed mechanism of galaxy formation in the cosmic string scheme, including baryons, must be investigated in the near future. Statistical properties of clusters of galaxies, such as the number density, mass function, and correlation function of clusters of galaxies (Dalton et al. 1992; Nicol et al. 1992; Bahcall & Cen 1992), are treated in a separate paper (Hara et al. 1994b).

We would like to point out that clusters of galaxies are accumulating dark matter still now vividly and that the cluster mass and average velocity dispersion increase even now (Edge et al. 1990). We have shown in Figure 11 the evolution of cluster mass and velocity dispersion for the typical case as described above. As far as the matter has not completely fallen into the wake which depends on the wake size, the cluster mass M, radius r, and velocity dispersion v_d of clusters increase as $M \propto a^3$, $r \propto a^2$, and $v_d \propto a^{0.5}$, as mentioned in § 4.

It is possible that galaxies are also formed at the crossing sites of three wakes at around the epoch $1 + z \simeq 8$. If the size of one or two wakes associated with the intersections of three wakes are much smaller than the size of $\sim 40\, h_{50}^{-1}$ Mpc (Hara et al. 1994b), they have already fallen toward the center or other wakes and the mass of galaxies seems to be partially saturated. However, as galaxies seem to be situated in a large wake as a great wall (Geller & Huchra 1989) or in a supercluster plane, dark matter may still fall into the wake and groups of galaxies therein (Hara & Miyoshi 1992).

For the explanation of the morphology of galaxies, we have to consider the crossing angles of three wakes and the limited size of each wake. For example, if the crossing site is situated near the edge of a crossing wake, the motion of dark matter toward the site is asymmetry and the accumulated dark matter system is expected to rotate. The preliminary calculations show that some dark matter systems rotate, although it is not large enough to explain the rotation curve of spiral galaxies. If we include the baryonic matter in the simulation of such asymmetrical contraction, the resultant configuration of baryonic matter and dark matter may be considerably different. It is possible that triaxial features could be understood in this scheme (Schweizer 1987; Davis 1989; de Zeeuw & Franx 1991). These are the subject of the next work (Hara et al. 1994a).

For a flattened or linear cluster of galaxies (Chapman, Geller, & Huchra 1988), it is necessary to investigate more general configuration of crossing angles of three wakes as well as velocity distribution of cosmic strings. It must be noted that there is a high possibility that clusters are situated within a wake or in a barlike intersected part of two wakes (Hara et al. 1994b), then a high rate of merging of these clusters is expected. This effect helps to make the exponent of the cluster-cluster correlation function near 2.

If galaxies were formed mainly in each wake and then fell to the gas-rich cluster center, the difference in the distributions for early-type and late-type galaxies and CDM in clusters could be explained (Ostriker et al. 1988). At any rate, we have to include the perturbation of CDM due to loops or initial fluctuation in our simulation, and a much more refined program, including the baryonic matter, is needed to follow the details of the inhomogeneity within a cluster of galaxies and the thermal history of the inter- and intra-cluster matter (Evrard 1990).

Finally we would like to note that the cosmic string model has a possibility to explain the observed anisotropy of the microwave background radiation (Smoot et al. 1992; Bennett, Bouchet, & Stebbins 1992; Perivolaropoulos 1993a, b; Hara et al. 1993b), the formation of large-scale structure of the universe (Vachaspati & Vilenkin 1991; Perivolaropoulos, Brandenberger, & Stebbins 1990; Vollick 1992; Hara, Mähönen, & Miyoshi 1993a) and the peculiar velocities of galaxies (Brandenberger et al. 1987; Vachaspati 1992; Hara et al. 1993c). Moreover, the formation of galaxies, globular clusters, and Lyα clouds might be explained by the string model (Hara et al. 1993a).

6. CONCLUSION

We have investigated the distribution of cold dark matter around a cluster of galaxies in the long cosmic string scheme. Although the adopted model is rather simple, we believe that some characteristic features of clusters of galaxies have been derived such as (1) the surface number density of galaxies around a cluster of galaxies, (2) the velocity dispersion of galaxies in a cluster of galaxies, and (3) the existence of a giant galaxy such as cD galaxy in the cluster center, having a similar shape with the host cluster.

Moreover our simulation shows that there is a characteristic length [$\sim 1.5(G\mu\beta\gamma/5 \times 10^{-6})$ Mpc] for cluster of galaxies and that clusters of galaxies are accumulating dark matter even now. The inhomogeneous distribution of dark matter within and around cluster of galaxies is also shown for a typical case, which is expected to be observed by X-ray telescope with fine angular resolution as intra- or intercluster substructures.

We would like to comment that, although cosmic strings with CDM and/or with HDM seem to give very promising and stimulating results, there are several "adiabatic" models which also give very impressive results and are regarded widely as a "standard theory." The reader should also remember that a stochastic probability of the configuration, where three cosmic string wakes cross each other perpendicularly is small (estimated to be $\sim 10^{-4}$ if we accept that $\Delta\theta < 15°$; Hara et al. 1994a). However, our aim is to study the structure formation with rather simple toy model and see what one can learn from that before going to make more realistic and complicated simulations.

One of the authors (T. H.) would like to thank H. Fujii and M. Toyama for their help in computation.

REFERENCES

Albrecht, A., & Turok, N. 1989, Phys. Rev., D40, 973
Allen, B., & Shellard, E. P. S. 1990, Phys. Rev. Lett., 64, 119
Bahcall, N. A., & Cen, R. 1992, ApJ, 398, L81
Batsuki, D. J., Mellot, A. L., Scherrer, R. J., & Bertschinger, E. 1991, ApJ, 367, 393
Beers, T. C., et al. 1991, AJ, 102, 1581
Beers, T. C., & Tonry, J. L. 1986, ApJ, 300, 557
Bertschinger, E. 1988, ApJ, 324, 5
Bennett, D., Bouchet, F., & Stebbins, A. 1992, ApJ, 399, L5
Binggeli, B. 1982, A&A, 107, 338
Bouchet, F., & Bennett, D. 1990, Phys. Rev., D41, 720
Bouchet, F., Bennett, D., & Stebbins, A. 1988, Nature, 335, 410
Brandenberger, R. 1990, in Clusters of Galaxies, ed. W. R. Oegerle et al. (Cambridge Univ. Press), 465
Brandenberger, R., Kaiser, N., Shellard, E. P. S., & Turok, N. 1987, Phys. Rev., D36, 335
Buote, D. A., & Canizares, C. R. 1992, ApJ, 400, 385
Cavaliere, A., & Colafracesco, S. 1990, in Clusters of Galaxies, ed. W. R. Oegerle et al. (Cambridge Univ. Press), 43
Chapman, G. N. F., Geller, M. J., & Huchra, J. P. 1988, AJ, 95, 999
Copeland, E., Kibble, T. W. B., & Austin, D. 1992, Phys. Rev., D45, 1000
Dalton, G. B., Efstathiou, G., Maddox, S. J., & Sutherland, W. J. 1992, ApJ, 390, L1
Davis, R. L. 1989, in The World of Galaxies, ed. H. G. Corwin & J. L. Bottinelli (New York: Springer), 312
Davis, D. S., & Mushotzky, R. F. 1993, AJ, 105, 409
de Vaucouleurs, G., et al. 1991, Third Reference Catalogue of Bright Galaxies (New York: Springer)
de Zeeuw, T., & Franx, M. 1991, ARA&A, 29, 239
Dressler, A. 1979, ApJ, 231, 659
Dressler, A., & Shectman, S. A. 1988, 95, 985
Edge, A. C., Stewart, G. C., Fabian, A. C., & Arnaud, K. A. 1990, MNRAS, 245, 559
Efstathiou, G., Davis, M., Frenk, C., & White, S. 1985, ApJS, 57, 241
Evrard, A. E. 1990, in Clusters of Galaxies, ed. W. R. Oegerle, M. J. Fitchett, & L. Danly (Cambridge Univ. Press), 287
Fitchett, M., & Webster, R. 1987, ApJ, 317, 653
Forman, W., & Jones, C. 1982, ARA&A, 20, 547
———. 1990, in Clusters of Galaxies, ed. W. R. Oegerle et al. (Cambridge Univ. Press), 287
Geller, M. J. 1990, in Clusters of Galaxies, ed. W. R. Oegerle, M. J. Fitchett, & L. Danly (Cambridge Univ. Press), 25
Geller, M. J., & Beers, T. C. 1982, PASP, 94, 421
Geller, M. J., & Huchra, J. P. 1989, Science, 246, 897
Hara, T., Mähönen, P., & Miyoshi, S. 1993a, ApJ, 412, 22
———. 1993b, ApJ, 414, 421
———. 1993c, ApJ, 415, 445
Hara, T., Matsuura, M., Yamamoto, H., Mähönen, P., & Miyoshi, S. 1994a, in preparation
Hara, T., & Miyoshi, S. 1989, Prog. Theor. Phys., 81, 1187
Hara, T., & Miyoshi, S. 1992, in Proc. 6th Marcel Grossman Meeting on General Relativity, ed. H. Sato & T. Nakamura (Singapore: World Scientific), 964
———. 1993, ApJ, 405, 419
Hara, T., Morioka, S., & Miyoshi, S. 1990, Prog. Theor. Phys., 84, 867
Hara, T., Yamamoto, H., Mähönen, P., & Miyoshi, S. 1994b, ApJ, in press
Hockney, R. W., & Eastwood, J. W. 1981, Computer Simulation Using Particles (New York: McGraw–Hill)
Hughes, J. P. 1989, ApJ, 337, 21
Kaiser, N. 1990, in Clusters of Galaxies, ed. W. R. Oegerle, M. J. Fitchett, & L. Danly (Cambridge Univ. Press), 327
Kent, S. M., & Gunn, J. E. 1982, AJ, 87, 945
Kibble, T. W. B. J. 1976, Phys., A9, 1387
McMillan, S. L. W., Kowalski, M. P., & Ulmer, M. P. 1989, ApJS, 70, 723
Millington, S. J. C., & Peach, J. V. 1986, MNRAS, 221, 15
Nicol, R. C., Collins, C. A., Guzzo, L., & Lumsden, S. L. 1992, MNRAS, 255, 21p
Ostriker, E. C., Huchra, J. P., Geller, M. J., & Kurz, M. J. 1988, AJ, 96, 1775
Peebles, P. J. E. 1990, in Clusters of Galaxies, ed. W. R. Oegerle, M. J. Fitchett, & L. Danly (Cambridge Univ. Press), 1
Peebles, P. J. E., & Silk, J. 1990, Nature, 346, 233
Perivolaropoulos, L. 1993a, Phys. Lett., 298, 305
———. 1993b, Phys. Rev., D48, 1530
Perivolaropoulos, L., Brandenberger, R., & Stebbins, A. 1990, Phys. Rev., D41, 1764
Quintana, H., & Lawrie, D. G., 1982, AJ, 87, 1
Sarazin, C. 1986, Rev. Mod. Phys., 58, 1
Sato, H. 1986, Prog. Theor. Phys., 75, 1342
Schweizer, F. 1987, in Structure and Dynamics of Elliptical Galaxies, ed. T. D. Zeeuw (Dordrecht: Reidel), 109
Shellard, E. P., & Allen, B. 1990, in The Formation and Evolution of Cosmic Strings, ed. G. W. Gibbons, S. W. Hawking, & T. Vachaspati (Cambridge Univ. Press), 421
Silk, J., & Vilenkin, A. 1984, Phys. Rev. Lett., 53, 1700
Smoot, G. F., et al. 1992, ApJ, 396, L1
Stebbins, A. 1988, ApJ, 327, 584
Stebbins, A., Veeraraghavan, S., Brandenberger, R., Silk, J., & Turok, N. 1987, ApJ, 322, 1
Tonry, J. L. 1985, AJ, 90, 2431
———. 1987, in Structure and Dynamics of Elliptical Galaxies, ed. T. D. Zeeuw (Dordrecht: Reidel), 89
Vachaspati, T. 1986, Phys. Rev. Lett., 57, 1655
———. 1992, Phys. Lett., B282, 305
Vachaspati, T., & Vilenkin, A., 1991, Phys. Rev. Lett., 67, 1057
Vilenkin, A. 1985, Phys. Lett., 121C, 263
Vollick, D. N., 1992, Phys. Rev., D45, 1884
West, M. J. 1990, in Clusters of Galaxies, ed. W. R. Oegerle, M. J. Fitchett, & L. Danly (Cambridge Univ. Press), 65
Yamashita, K. 1992, in Frontiers of X-Ray Astronomy, ed. Y. Tanaka & K. Koyama (Tokyo: Universal Academy), 475